Supporting Information

Effect of macromolecular crowding on the kinetics of glycolytic enzymes and the behaviour of glycolysis in yeast

Henrik S. Thoke[a,b], Luis A. Bagatolli[c], and Lars F. Olsen[*a,b]

[a]MEMPHYS - international and interdisciplinary research network ; [b]Institute for Biochemistry and Molecular Biology, University of Southern Denmark, Campusvej 55, DK5230 Odense M,Denmark

[c]Instituto de Investigación Médica Mercedes y Martin Ferreyra (INIMEC-CONICET-Universidad Nacional de Córdoba), Friulli 2434, X5016NST Córdoba, Argentina.
*Correspondence and requests should be addressed to lfo@bmb.sdu.dk

Supporting Methods

Chemicals

6-Propionyl-2-(dimethylamino)naphthalene (PRODAN) and 6-lauroyl-2-(dimethylamino)naphthalene (LAURDAN), and Nile Red were obtained from Invitrogen (Denmark).

Yeast strains and growth

The yeast strains used in this study were obtained from EUROSCARF (Frankfurtam Main, Germany) and grown as previously described.[1]

Generation of glycolytic oscillations

Unlabeled or fluorescently labeled yeast cells at 10% (w/v) in 100mM phosphate buffer, pH 6.8, were added to a 2mL cuvette mounted in the spectrofluorometer under stirring. Glycolityc oscillations were induced by first adding 30 μL from a 2 M stock solution of glucose to reach a concentration in the sample of 30 mM and then (60 s later) 20 μL from a 0.5 M stock solution of KCN to reach a concentration in the sample of 5 mM.

Staining of cells with ACDAN, PRODAN, LAURDAN and Nile Red

Stock solutions of ACDAN, PRODAN, LAURDAN and Nile Red in $\geq$ 99 % DMSO of 1-2 mM were prepared. Yeast cells (10% w/v) in 100mM potassium phosphate buffer, pH 6.8, were incubated at 30 °C with either 10μM ACDAN, 10μM PRODAN or 20μM LAURDAN and 5μM Nile Red for 0:5h-1:5h. The cells were then washed with the same buffer, centrifuged at 6000 g and finally resuspended in 100mM potassium phosphate buffer, pH 6.8

Fluorescence measurements

Measurements of NADH, ACDAN, PRODAN, LAURDAN and Nile Red fluorescence were performed using a QE65000 spectrometer (Ocean Optics, Dunedin, FL) fitted with a temperature-controlled cuvette holder (Quantum Northwest, Liberty Lake, WA, USA). The sample temperature was maintained at 25°C unless otherwise stated. Excitation light was supplied by a CoolLED pE-4000 illumination system (CoolLED, Andover, UK). The optical fiber from the illumination system was mounted perpendicular to the emission beam. NADH was excited at 365nm (10nm width at half height), and fluorescence emission was measured as the average intensity in the wavelength range 435nm⊡450nm. ACDAN, PRODAN and LAURDAN were excited at 365nm (10nm width at half height), and fluorescence emission was measured as the average intensity in the wavelength range 435nm-445nm. Nile Red fluorescence was excited at 525nm (10nm width at half height).
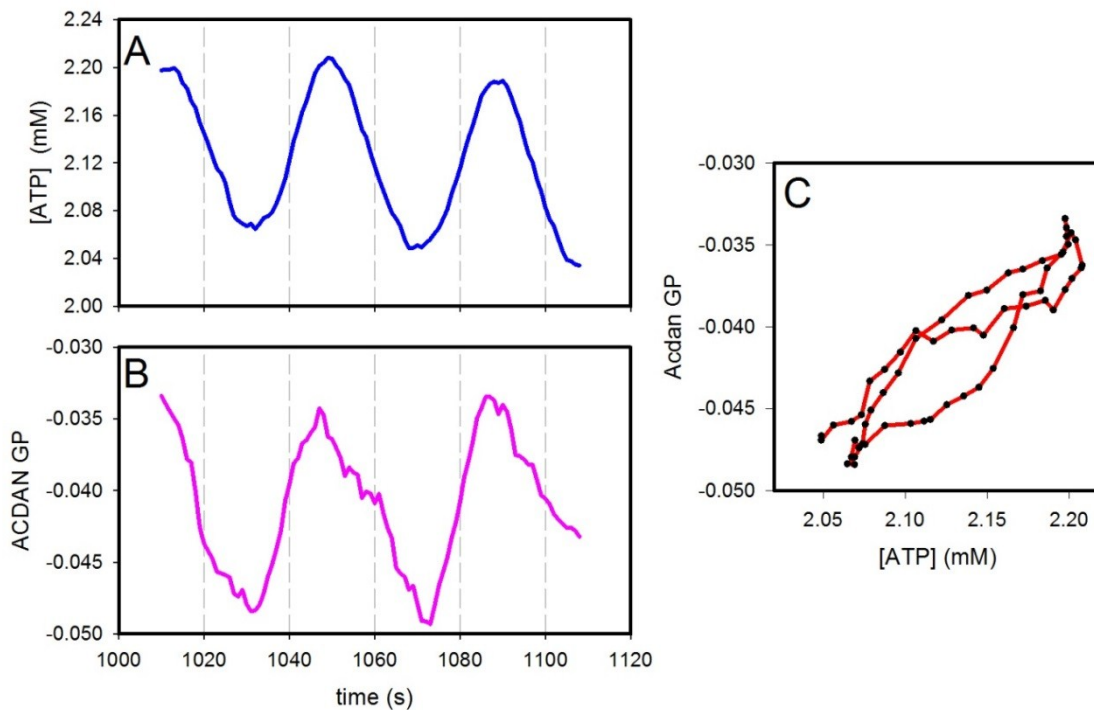
Figure S1 Oscillations in intracellular ATP and ACDAN GP in *S. cerevisiae* cells grown at 30 °C. (A) and (B) time series of ATP and ACDAN GP; (C) phase plot of ACDAN GP versus intracellular ATP. Yeast cells (10% w/v) were suspended at 25 °C in 100 mM potassium phosphate, pH 6.8 and oscillations were induced by addition of glucose (final concentration 30 mM) and 60 s later KCN (final concentration 5 mM). ACDAN GP was measured as described in (10) Intracellular ATP concentration was measured using an aptamer-based ATP nanosensor[2] inserted into the cells using electroporation.
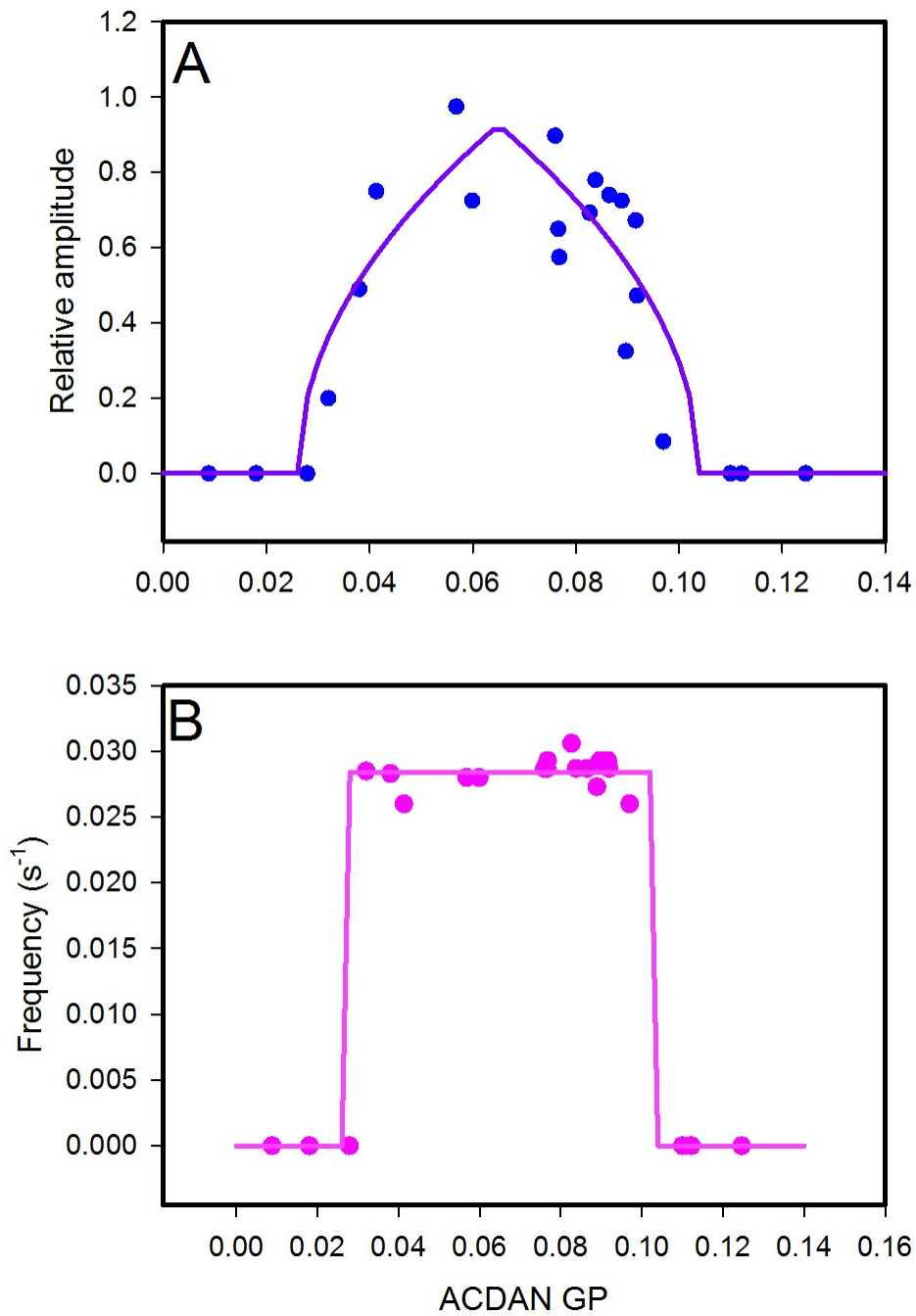
Figure S2 Plots of the glycolytic (NADH) oscillation amplitude (A) and the frequency (B) against the ACDAN GP of the wild type (S. cerevisiae BY4743) and 21 strains with isogenic mutations of various proteins in glycolysis, ATPase activity (F_1F_0 and vacuolar ATPase), actin polymerization and microtubule formation. All strains were grown at 30 °C and measured at 25 °C. The oscillation amplitude is scaled relative to the amplitude of NADH oscillations of the wild type strain (S. cerevisiae BY4743) (For further details see ref. (3)). The solid curves represent two supercritical Hopf bifurcations.[3]
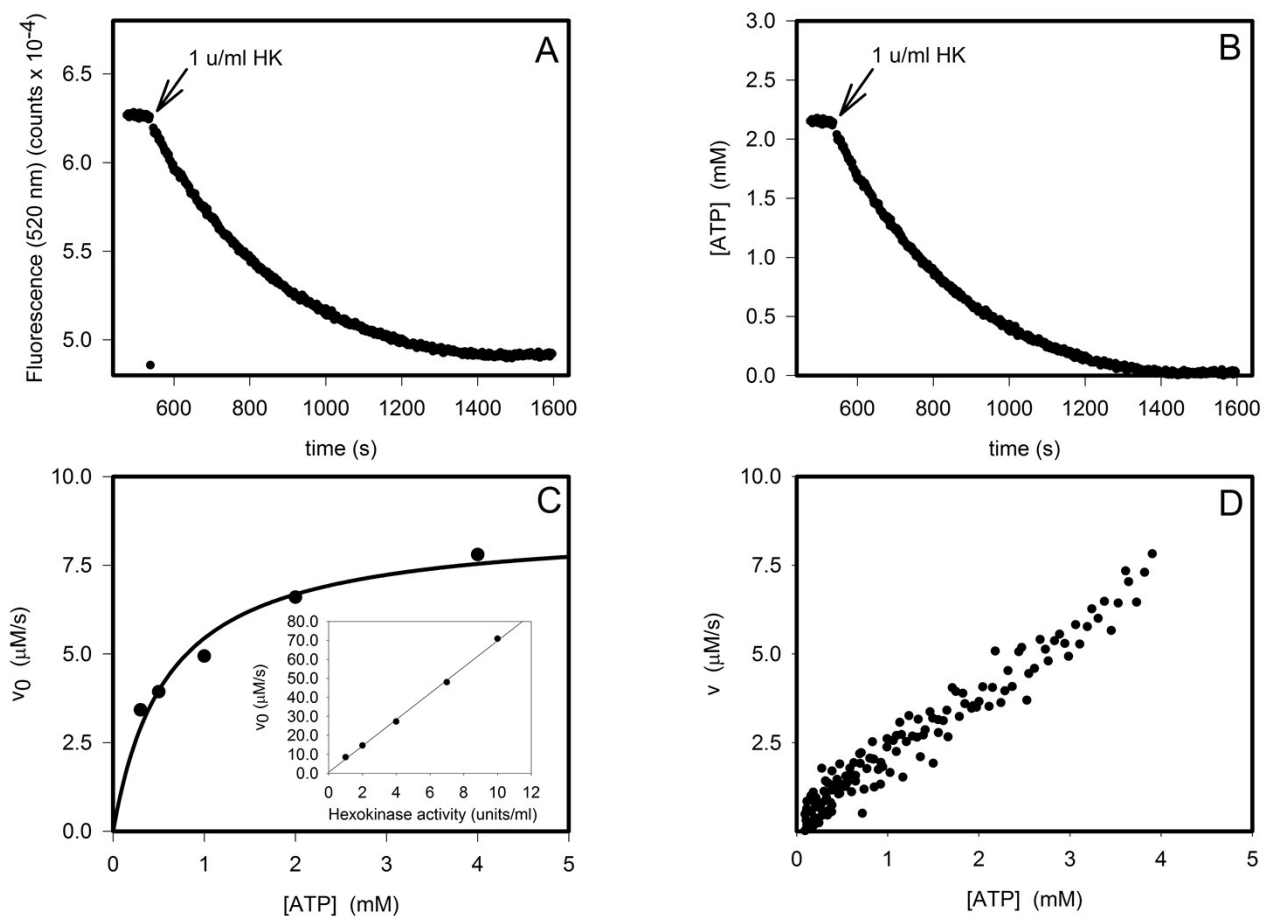
Figure S3. Kinetics of yeast hexokinase. A, Recording of fluorescence due to Alexa Fluor 488 on the ATP sensor with excitation at 470 nm and emission at 520 nm. 2 mM ATP is added to a 2 ml solution containing 10 mM potassium phosphate, pH 7.0, 50 mM Na_2SO_4, 5 mM $MgCl_2$, 10 mM glucose and ATP sensor corresponding to 1 mg/ml. At the arrow 1 unit of hexokinase (HK) was added to the solution and the fluorescence decreases due transfer of phosphate from ATP to glucose. Temperature 25 ± 0.01 °C. B, Same experiment as in A, but here the fluorescence at 520 nm was converted to ATP concentration by using a sensor calibration curve (not shown). C, Plot of initial rate v_0 of ATP consumption calculated from progress curves like than in B against ATP concentration. The inset shows the initial rate of ATP consumption plotted against the concentration of added hexokinase (in units/ml) for an initial ATP concentration of 4 mM. D, Plot of the instantaneous rate of ATP consumption, calculated as the slope of the progress curve like that in B but with initial ATP concentration of 4 mM, against the ATP concentration.
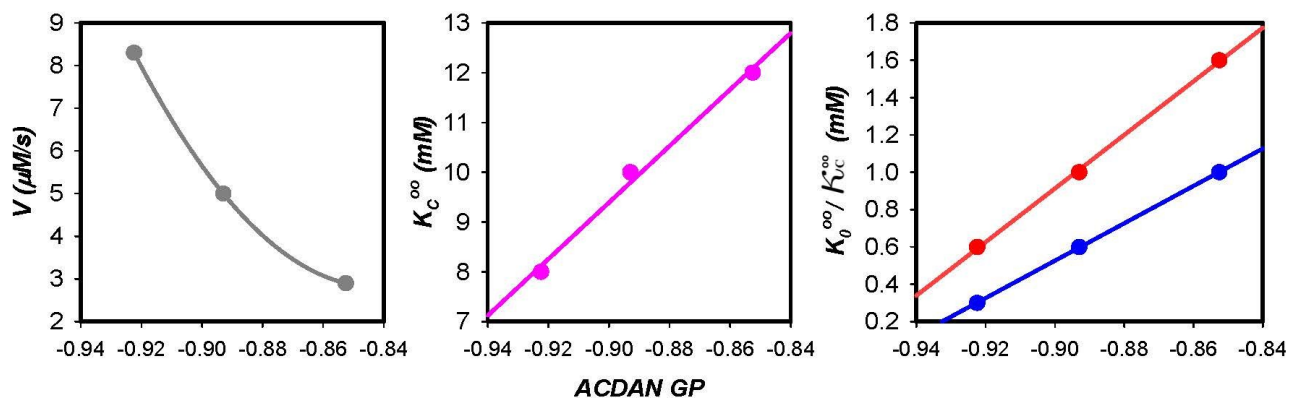
Figure S4 Plot of the parameters V (gray), K_C^{oo} (violet), K_0^{oo} (blue) and κ_C^{oo} (red) for HK (Table 1 in the main text) against the ACDAN GP for aqueous solutions with 0, 10% and 30% PEG. ACDAN GP is evaluated from spectra of ACDAN as $(I_{450}-I_{490})/(I_{450}+I_{490})$.[3,4]
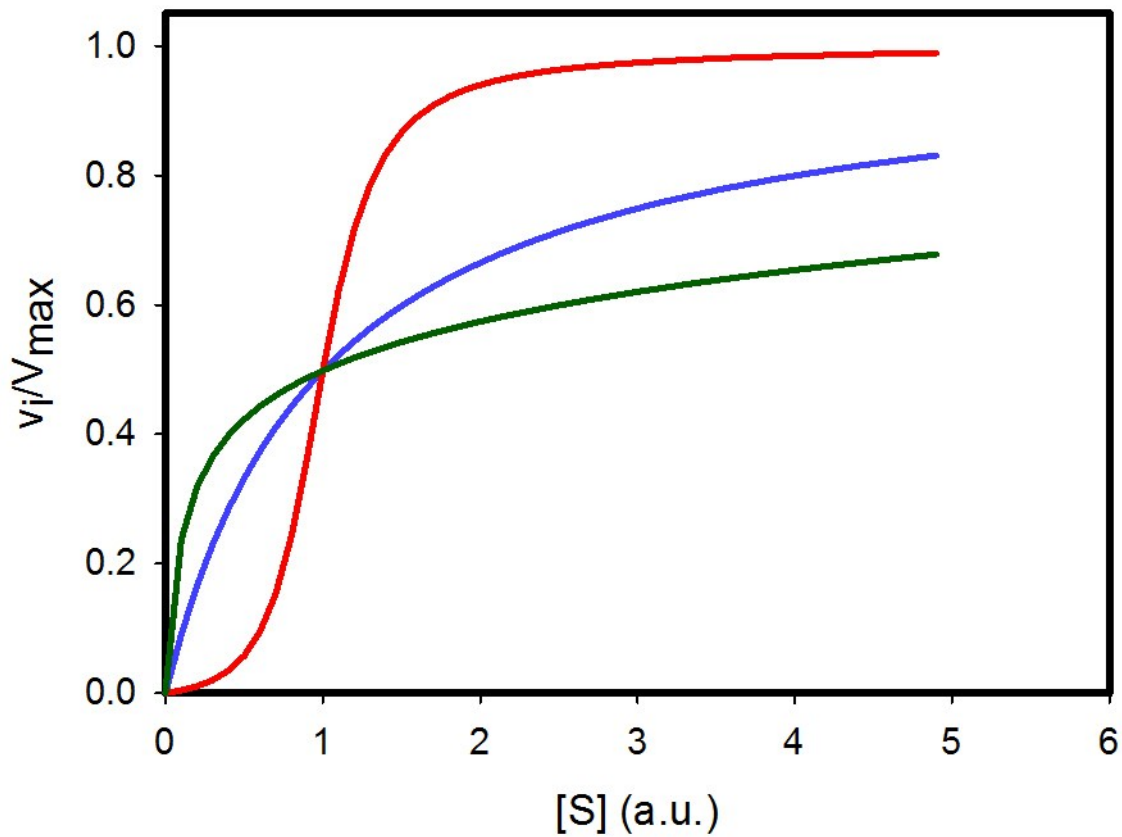
Figure S5 Cooperative and non-cooperative behaviour of the Yang-Ling isotherm. The graphs are made using equations (13)-(14) in the main text and omitting a cardinal absorbent with the following parameters $K_c^{oo} = 10$; $-\dfrac{\gamma_c}{2} =$ 1.0 kcal/mol; $K_o^{oo} = 1$; $-\dfrac{\gamma_o}{2} =$ 0.0 kcal/mol (blue) , 1 kcal/mol (red) or -0.5 kcal/mol (green).

The steepness of the red graph is determined by the size of $-\dfrac{\gamma_o}{2}$. The larger the size the higher is the maximum slope of that graph. If $-\dfrac{\gamma_o}{2}$ becomes negative we obtain negative cooperativity.
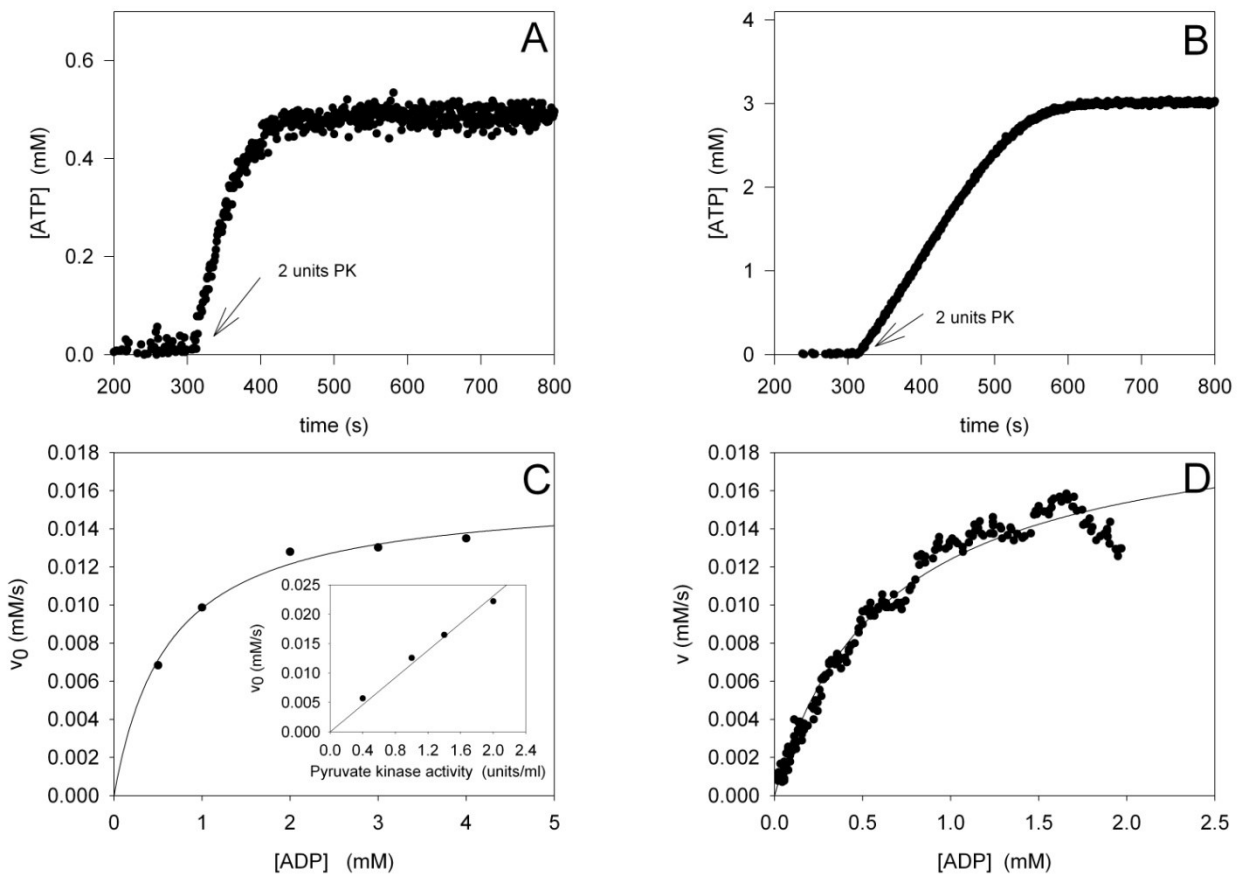
Figure S6. Kinetics of rabbit muscle pyruvate kinase. A,B Progress curves of ATP formation after adding 2 *U* of pyruvate kinase (PK) to a 2 ml solution containing 10 mM potassium phosphate, pH 7.0, 50 mM Na_2SO_4, 5 mM $MgCl_2$, 10 mM phosphoenolpyruvate (PEP), 0.5 mM ADP (A) or 3 mM ADP (B) and ATP sensor corresponding to 2 mg/ml. Temperature 25 ± 0.01 °C. C, Plot of the initial rate v_0 of ATP formation, determined from progress curves like those in Fig 4A and 4B, against concentration of ADP. The inset shows a plot of v_0 against the concentration of added pyruvate kinase (in units/ml) for an initial ADP concentration of 2 mM. D, Plot of the instantaneous rate of ATP formation, calculated as the derivative of progress curves like those in Fig. 4A and 4B but with initial ADP concentration of 2 mM, against the ADP concentration.
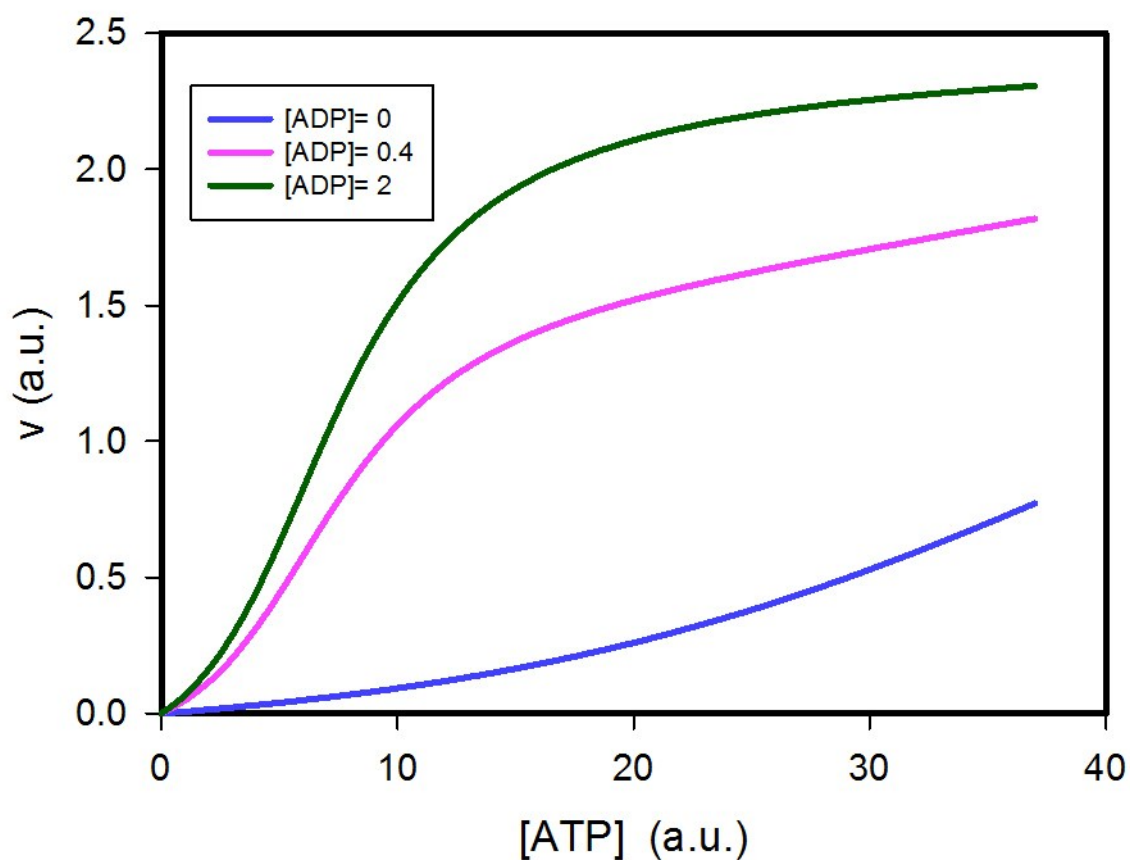
Figure S7 Plots of v against [ATP] at different concentrations of ADP for PFK using the Yang-Ling isotherm model (Equations (17), (14) and (15) in the main text). Concentrations of ADP (dimensionless) are 0 (blue), 0.4 (violet) and 2 (dark green). Parameters (most of them dimensionless) are: V=2.5; $K_c^{oo} = 8$; $-\frac{\gamma_c}{2} = 0.5$ kcal/mol; K_o^{oo} =50; $-\frac{\gamma_o}{2} = 0.6$ kcal/mol; $\kappa_c^{00} = 10$; $-\frac{\Gamma}{2} = 0.7$ kcal/mol.
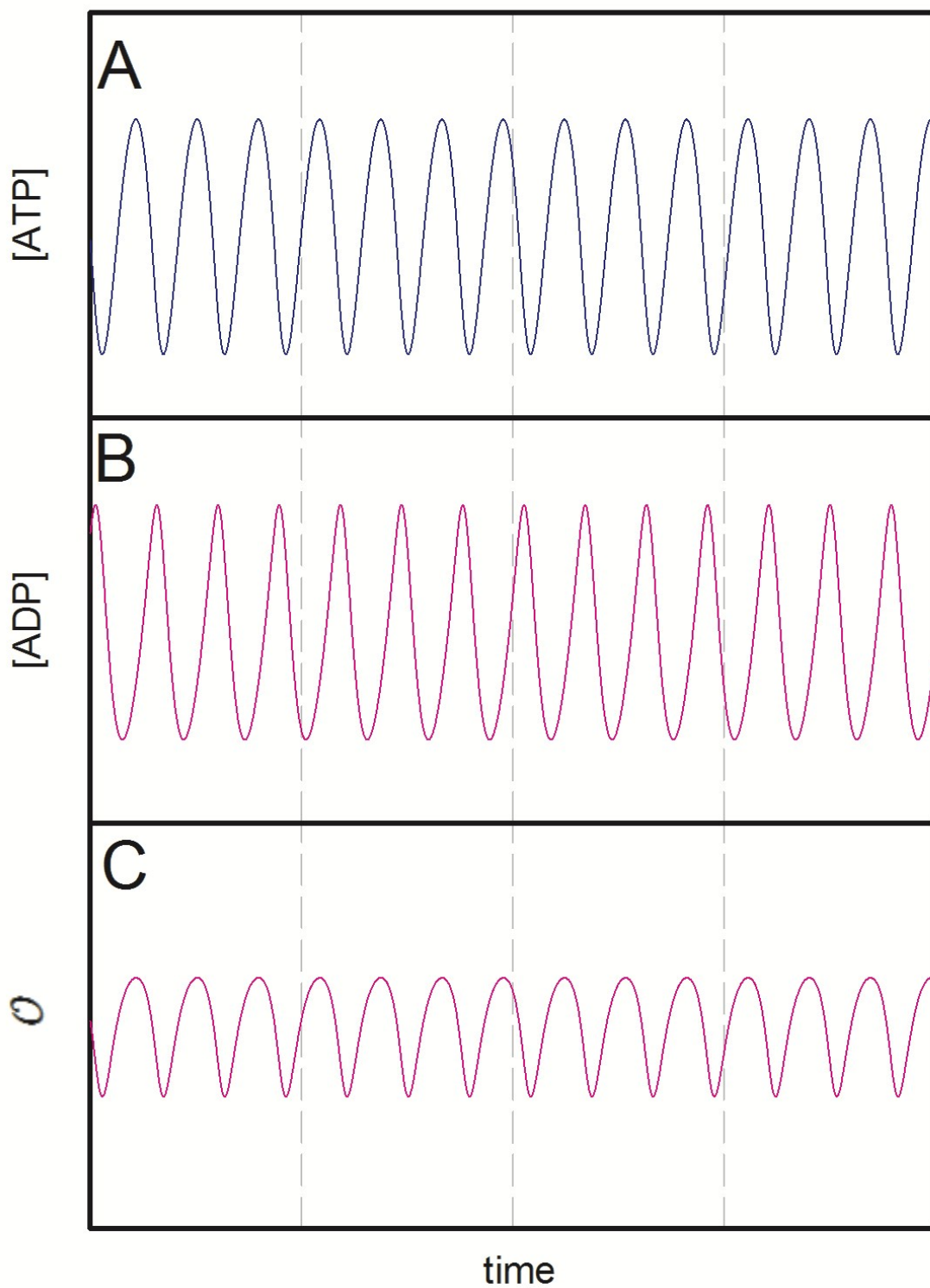
Figure S8 Simulations of equations (18), (19) and (21) in the main text. Plots of concentrations of ATP, ADP and $\mathcal{O}$ against time. Parameters as in Fig. 4 in the main text.
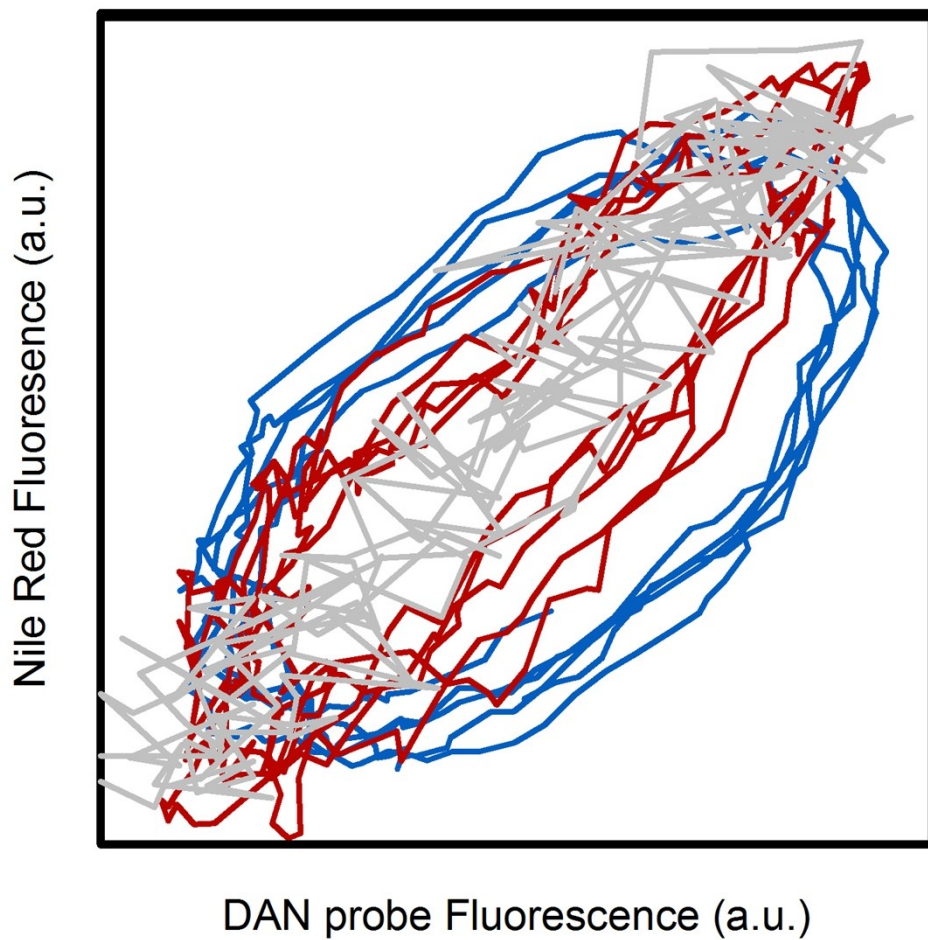
Figure S9. Experimental phase plot of the fluorescence intensities of Nile Red versus the DAN probes: ACDAN versus Nile Red (blue), PRODAN versus Nile Red (red) and LAURDAN versus Nile Red (grey).

References

1. V.C. Özalp, L.J. Nielsen, and L.F Olsen**.** An aptamer-based nanobiosensor for real-time measurements of ATP dynamics. *ChemBioChem*, 2010, 11, 2538-2541

2. T.D. Schrøder, V.C. Özalp, A. Lunding, K.D. Jernshøj and L.F. Olsen**.** An experimental study of the regulation of glycolytic oscillations in yeast. *FEBS J.*, 2013, 280, 6033–6044.

3. H.S. Thoke, A. Tobiesen, J. Brewer, P.L. Hansen, R. P. Stock, L.F. Olsen and L.A. Bagatolli. Tight coupling of metabolic oscillations and intracellular water dynamics in *Saccharomyces cerevisiae*. *PLoS One*, 2015, 10(2): e0117308.

4. H.S. Thoke, S. Thorsteinsson, R.P. Stock, L.A. Bagatolli and L.F. Olsen. The dynamics of intracellular water constrains glycolytic oscillations in *Saccharomyces cerevisiae. Sci. Rep.*, 2017, 7:16250.